Effect of nodes, ellipticity, and impurities on the spin resonance in iron-based superconductors

S. Maiti, J. Knolle, I. Eremin, and A.V. Chubukov

Effect of nodes, ellipticity and impurities on the spin resonance in Iron-based superconductors

S. Maiti[1], J. Knolle[2], I. Eremin[3] and A.V. Chubukov[1]

[1] *Department of Physics, University of Wisconsin-Madison, Madison, Wisconsin 53706, USA*
[2] *Max-Planck-Institut für Physik komplexer Systeme, D-01187 Dresden, Germany*
[3] *Institut für Theoretische Physik III, Ruhr-Universität Bochum, D-44801 Bochum, Germany*
(Dated: September 30, 2011)

We analyze doping dependence of the spin resonance of an $s^{\pm}$ superconductor and its sensitivity to the ellipticity of electron pockets, to magnetic and non-magnetic impurities, and to the angle dependence of the superconducting gap along electron Fermi surfaces. We show that the maximum intensity of the resonance shifts from commensurate to incommensurate momentum above some critical doping which decreases with increasing ellipticity. Angle dependence of the gap and particularly the presence of accidental nodes lowers the overall intensity of the resonance peak and shifts its position towards the onset of the particle-hole continuum. Still, however, the resonance remains a true $\delta-$function in the clean limit. When non-magnetic or magnetic impurities are present, the resonance broadens and its position shifts. The shift depends on the type of impurities and on the ratio of intraband and interband scattering components. The ratio $\Omega_{res}/\mathrm{T}_c$ increases almost linearly with the strength of the interband impurity scattering, in agreement with the experimental data. We also compare spin response of $s^{\pm}$ and s^{++} superconductors. We show that there is no resonance for s^{++} gap, even when there is a finite mismatch between electron and hole Fermi surfaces shifted by the antiferromagnetic momentum.

I. INTRODUCTION

The relation between unconventional superconductivity and magnetism is one of the most interesting topics in condensed-matter physics. In conventional phonon- mediated $s-$wave superconductors (SCs), the SC gap Δ is approximately a constant along the Fermi surface (FS), and paramagnetic spin excitations at $T << T_c$ are suppressed below 2Δ due to formation of Cooper pairs with the total spin $S = 0$. In unconventional SCs, such as layered cuprates or some heavy fermion materials, the pairing symmetry is $d-$wave, and the SC gap changes sign along the Fermi surface. In this situation, the suppression of the spin response is only one effect of superconductivity, another is the appearance of the resonance below the onset of the particle-hole continuum, at a set of momenta which connect FS points with different signs of the gap.[1]. The intensity of the resonance is the strongest at $\mathbf{Q}$ for which the gap magnitude is the largest at the corresponding FS points. For many unconventional SCs such $\mathbf{Q}$ coincides with the antiferromagnetic momentum (π, π).

In general, the spin resonance has contributions from both fermionic excitations in particle-hole and particle-particle channels, which are mixed in a superconductor.[2] In most cases, however, the dominant contribution to the resonance comes from particle-hole channel and from this perspective the resonance can be viewed as a spin exciton[3]. The spin resonance is a true $\delta-$function in a 2D superconductor at $T = 0$, but acquires a finite width at a finite T in 2D, and even at $T = 0$ in 3D systems[4], if a line of nodes intersects the locus of FS points separated by $\mathbf{Q}$. A broadened resonance survives even when the

system loses superconducting phase coherence[5], *i.e.*, it still exists in some T range above T_c, however its intensity sharply increases only below T_c.

Because spin resonance only develops when there is a sign change of the superconducting gap between $\mathbf{k}_F$ and $\mathbf{k}_F + \mathbf{Q}$, it is widely regarded as a probe of unconventional gap symmetry or structure, complementary to phase sensitive measurements. The observation of the spin resonance in the cuprates[6] and in some heavy-fermion materials [7,8] is a strong evidence of a $d-$wave gap symmetry in these materials.

The subject of this paper is the analysis of the several features of the spin resonance seen by inelastic neutron scattering (INS) in Fe-based superconductors (FeSCs). These systems are multi-orbital/multi-band metals with two or three hole FS pockets centered at the Γ point $(0,0)$ and two elliptical electron FS pockets centered at (π, π) in the actual, folded Brillouin zone (BZ) with 2 $Fe-$ atoms per unit cell. There also exist FeSCs with only hole or only electron FSs, but we will not discuss these materials. Throughout this paper we assume that FeSCs can be reasonably well approximated by 2D models and neglect the anisotropy of electron dispersion along k_z. We also consider only interactions that conserve momentum in the unfolded BZ (1 $Fe-$ atoms per unit cell) and neglect additional interactions via a pnictogen, which only conserve momentum in the folded BZ and hybridize the two electron pockets. This hybridization is relevant to systems with only electron FSs[9], but does not look to be important for our consideration.

Angle Resolved Photoemission Spectroscopy (ARPES) studies of FeSCs with hole and electron pockets demonstrated quite convincingly that the SC gap in these sys-

tems does not have nodes along the hole FSs, at least for k_z probed by ARPES. The absence of the nodes is the proof that FeSCs are $s-$wave superconductors, otherwise the gap would have nodes on hole pockets for all k_z. Still, however, in a multi-band SC, $s-$wave gap can be unconventional and give rise to the spin resonance in INS. Indeed, s-wave symmetry only implies that the SC gap is approximately a constant along hole FSs, but does not impose a restriction on the relative signs of the SC gaps along hole and electron FSs separated by $\mathbf{Q}$. A gap structure consistent with ARPES can be either a conventional, sign-preserving s^{++} gap, or an unconventional $s^{\pm}$ gap which changes sign between hole and electron FSs.

Both gaps have been proposed for FeSCs based on the two different assumptions about the interplay between intra-orbital and inter-orbital screened Coulomb interactions. $s^{\pm}$ gap has been proposed based on the assumption that intra-orbital interaction is stronger than the inter-orbital one. In the band description, this condition implies that both intra-pocket and inter-pocket interactions are positive, i.e., repulsive. Then a conventional $s-$wave superconductivity is impossible, but $s^{\pm}$ pairing is possible if the inter-pocket is larger than the intra-pocket one. A positive inter-pocket interaction is enhanced by antiferromagnetic fluctuations and close enough to a magnetic instability overcomes intra-pocket repulsion[10–17]. The same antiferromagnetic fluctuations also enhance a d-wave pairing component, but a d-wave gap has nodes on the hole FSs and has a smaller condensation energy, at least near a magnetic transition.

The alternative, s^{++} pairing has been proposed[18] based on the opposite assumption that intra-orbital interaction is weaker than the inter-orbital one. In the band description, this implies that intra-pocket interaction is repulsive (positive), but inter-pocket interactions is attractive (negative). Then a conventional s^{++} superconductivity occurs once inter-pocket interaction exceeds the intra-pocket one. A negative inter-pocket pairing interaction is enhanced by charge (orbital) fluctuations in combination with phonons, that is, if orbital fluctuations play the dominant role, the system develops an s^{++} superconductivity.

Because $s^{\pm}$ gap changes the sign between hole and electron FSs, it satisfies the same condition for the resonance, $\Delta_{\mathbf{k}} = -\Delta_{\mathbf{k+Q}}$ as in a $d-$wave superconductor. Accordingly, the spin response of an $s^{\pm}$ superconductor below T_c should contain a sharp, nearly $\delta-$functional spin resonance[19–21]. No such resonance develops if the gap is a conventional s^{++} structure.

The peak in the dynamical spin susceptibility has been observed below T_c at the antiferromagnetic wave vector $\mathbf{Q}$ in several FeSCs [22–24] and has been regarded by many as the strong, yet indirect experimental evidence in favor of $s^{\pm}$ gap. [Other indirect evidences for $s^{\pm}$ SC are the observation of a magnetic field dependence of the quadripartite interference peaks in STM[25] and the very presence of the co-existence phase between antiferromagnetism and SC[26]]. These experimental findings are particularly important because direct phase sensitive measurements of the gap in FeSCs are lacking.

Another interpretation of the magnetic peak was put forward by Kontani and his collaborators [27]. They argued that, even in an s^{++} superconductor, there is a redistribution of a magnetic spectral weight below T_c due to the opening of a spin gap. This by itself leads to the development of a peak in the differential dynamical spin susceptibility (the one below T_c minus the one at T_c). This peak is not a resonance and occurs above 2Δ, contrary to the resonance which is a true bound state and as such must be located below 2Δ. In principle, this difference should be sufficient to determine which scenario is consistent with the data, particularly given that the gaps have been measured by ARPES. The difficulty, however, is that FeSCs have several gaps of different magnitudes, and the measured position of the peak in the magnetic response is below $2\Delta_{max}$ but above $2\Delta_{min}$ and hence can be interpreted both ways[28]

In this paper, we analyze in detail other properties of the spin resonance peak in FeSCs which could help establish more accurately whether or not the development of the peak in the spin response below T_c is the evidence for $s^{\pm}$ gap. For this, we explore in detail similarities and differences between the resonance in FeSCs and the resonance in d-wave cuprate superconductors.

The spin resonance in the cuprates has been studied in great detail over the last 15 years. The FS in the cuprates is large and both $\mathbf{k}_F$ and $\mathbf{k}_F + \mathbf{Q}$ are on the same FS sheet (these special points are called hot spots). The velocities at the two hot spots separated by $\mathbf{Q}$ are neither parallel not antiparallel, such that the original FS and the shadow one, with $\mathbf{k}$ shifted by $\mathbf{Q}$, simply cross at a hot spot. In this situation, the sign change of the gap between the two hot spots separated by $\mathbf{Q}$ implies that the imaginary part of the bare particle-hole susceptibility $\text{Im}\chi_0(\mathbf{Q}, \Omega)$ jumps at 2Δ from its zero value below 2Δ to a finite value immediately above 2Δ. By Kramers-Kronig relation, the real part of the particle-hole susceptibility $\text{Re}\chi_0(\mathbf{Q}, \Omega)$ then diverges logarithmically at 2Δ. Because $\text{Re}\chi_0(\mathbf{Q}, 0)$ changes only little between the normal and the SC state and $\text{Re}\chi_0(\mathbf{Q}, \Omega)$ diverges upon approaching 2Δ from below, the full susceptibility $\chi(\mathbf{Q}, \Omega) \propto (1 - U\chi_0(\mathbf{Q}, \Omega))^{-1}$ develops a $\delta-$functional resonance at some $\Omega_{res}(\mathbf{Q}) < 2\Delta$, where $\text{Im}\chi_0(\mathbf{Q}, \Omega) = 0$. Upon momentum deviations from $\mathbf{Q}$, $\chi_0(\mathbf{q} + \mathbf{Q}, \Omega)$ decreases chiefly due to the momentum variation of the d-wave gap. The resonance frequency approaches zero at $\mathbf{q} + \mathbf{Q}$ equal to the distance between the two opposite points on the FS where the $d-$wave gap vanishes. [At even larger $\mathbf{q}$ the new, second resonance develops and the resonance frequency bounces back[29].]

In FeSCs, the physics behind the resonance is similar to the one in the cuprates in the sense that the sign change of the gap between hole and electron FSs again gives rise to the divergence of the particle-hole susceptibility at 2Δ. But there are also two important differences. First, an $s-$wave gap does not induce a downward dispersion of

the resonance. Second, the resonance in FeSCs is more likely to become incommensurate either upon doping or even at zero doping. This happens because the geometry of electron and hole FSs in FeSCs is such that there exist special momenta $\mathbf{q} \neq 0$, at which a hole FS shifted by $\mathbf{q}+\mathbf{Q}$ just touches an electron FS. At these special $\mathbf{q}$, the real part of the particle-hole susceptibility diverges as $(2\Delta - \Omega)^{-1/4}$, *i.e.* stronger than logarithmically. These $\mathbf{q}$ appear at a finite doping if all FSs are approximated by circles and exist already at zero doping if we treat electron FSs as elliptical. Because the stronger is the divergence, the farther down is the resonance from 2Δ, the position of the lowest Ω_{res} shifts, upon increasing doping or ellipticity, from a commensurate $\mathbf{Q}$ to an incommensurate $\mathbf{q}+\mathbf{Q}$, with a non-zero $\mathbf{q}$. We show that the intensity of the resonance does not follow this shift instantly, but eventually the intensity also becomes the strongest at an incommensurate $\mathbf{q} + \mathbf{Q}$. A transformation from a commensurate to an incommensurate spin resonance upon doping has been found in the recent neutron study of the evolution of the resonance in $Ba_{1-x}K_xFe_2As_2$ with doping[30]. An incommensurate spin resonance has been observed in Ref. 31 in a superconducting $FeTe_{0.6}Se_{0.4}$.[32]

We also discuss in detail the width of the resonance peak in FeSCs. Experimentally, the peak is quite broad already at low T, which was argued[27] to be inconsistent with a true resonance. We show that there are two effects, specific to FeSCs, which lead to additional broadening of the peak. First is the symmetry-imposed $\cos 2\theta$ angle variation of the gap along electron FSs, the second is pair-breaking effect on $s^\pm$ superconductivity from non-magnetic impurities which scatter between hole and electron FSs.

We show that the impurity scattering broadens the resonance peak, but its position, i.e. Ω_{res}, remains essentially unaffected. Given that T_c decreases by impurity scattering, the ratio Ω_{res}/T_c increases with increasing impurity concentration which correlates with the increase of doping. This trend is in agreement with recent INS experiments[30] which show that Ω_{res}/T_c moves up with increasing doping.

The two key conclusions of our study is that (i) the doping dependence and the shape of the spin resonance in FeSCs is fully consistent with the $s^\pm$ gap structure, and (ii) the spin response of an $s^\pm$ SC can be fully understood within an itinerant approach, without invoking any localized moments.

For completeness, we also discuss one particular aspect of the interplay between magnetic responses at $\mathbf{Q}$ in s^{++} and $s^\pm$ superconductors. Namely, previous calculations have demonstrated that there is no true resonance in an s^{++} superconductor, when the original and the shadow FSs cross. We verify what happens with the resonance when the original and the shadow FSs do not cross, which is the case when both hole and electron FSs are near-circular and the doping is finite, such that one FS is larger than the other. In this situation, the onset of particle hole continuum in $Im\chi_0(\mathbf{Q},\Omega)$ shifts upwards

from 2Δ. We find that, even in this case, there is no resonance for s^{++} gap (and there is the resonance for $s^\pm$ gap). The only feature that emerges for s^{++} gap is a broad maximum in $Im\chi(\mathbf{Q},\Omega)$ above 2Δ. Whether this rules out s^{++} gap as the explanation for neutron data is a more subtle issue because the width of $Im\chi(\mathbf{Q},\Omega)$ in an s^{++} superconductor depends on system parameters and, quite possibly, on the fermionic self-energy and its evolution below T_c (Refs. 27,28).

The paper is organized as follows. In Sec. II we introduce the model and discuss the computation of a spin susceptibility in a multi-band superconductor. In Sec. III we discuss the doping dependence of the resonance, doping-induced incommensuration, the role of ellipticity of the electron pockets, the role of the angle variation of the gap as well as one particular aspect of the interplay between magnetic responses at $\mathbf{Q}$ in s^{++} and $s^\pm$ superconductors. In Sec. IV we discuss how the resonance is affected by non-magnetic impurities, which are pair-breaking for $s^\pm$ gap. Results with magnetic impurities are also included. Our concluding remarks are presented in Sec. V

II. THE MODEL

We start from the 4-band model with two circular hole pockets at $(0,0)$ (α-bands) and two elliptic electron pockets at $(\pi,0)$ and $(0,\pi)$ points in the unfolded Brillouin Zone (UBZ) (β-bands). The quadratic part of the Hamiltonian is

$$H_2 = \sum_{\mathbf{p},\sigma,i=1,2}\left[\varepsilon_\mathbf{p}^{\alpha_i}\alpha_{i\mathbf{p}\sigma}^\dagger\alpha_{i\mathbf{p}\sigma} + \varepsilon_\mathbf{p}^{\beta_1}\beta_{1\mathbf{p}\sigma}^\dagger\beta_{1\mathbf{p}\sigma} + \varepsilon_\mathbf{p}^{\beta_2}\beta_{2\mathbf{p}\sigma}^\dagger\beta_{2\mathbf{p}\sigma}\right].(1)$$

To facilitate numerical calculations, we consider lattice dispersions for all four bands, although the resonance essentially comes only from fermionic states near the FSs. We set $\varepsilon_\mathbf{p}^{\alpha_i} = t_\alpha\left(\cos p_x + \cos p_y\right) - \mu_i$ and $\varepsilon_\mathbf{p}^{\beta_1} = \epsilon_0 + t_\beta\left([1+\epsilon]\cos(p_x+\pi) + [1-\epsilon]\cos(p_y)\right) - \mu_1$, $\varepsilon_\mathbf{p}^{\beta_2} = \epsilon_0 + t_\beta\left([1-\epsilon]\cos(p_x) + [1+\epsilon]\cos(p_y+\pi)\right) - \mu_1$. The momenta are measured in units of inverse Fe-Fe spacing $a_x = a_y = a$. The parameter ϵ accounts for the ellipticity of the electron pockets. To make qualitative comparisons to experiments, we set Fermi velocities and Fermi surfaces to be equal to those in Refs. 33,34 For this we take $t_\alpha = 0.85eV$, $t_\beta = -0.68eV$, $\mu_1 = 1.54eV$, $\mu_2 = 1.64eV$, and $\epsilon_0 = 0.31eV$. For $\epsilon = 0.8$ the Fermi velocities are $0.5eVa$ for the two degenerate α-bands, and $v_x = 0.27eVa$ and $v_y = 0.49eVa$ along x- and y-directions for the β_1-band (and vice versa for the β_2 band) [see Ref.35]. The Fermi surfaces are shown in Fig. 1(a).

The interacting part of the Hamiltonian contains four-fermion interactions with small momentum transfer and momentum transfers $(\pi,0)$, $(0,\pi)$, and (π,π). They include $\alpha - \beta$ interactions with momentum transfer $(0,\pi)$

and $(\pi, 0)$ as well as β-β and α-α interactions with momentum transfers $(0,0)$ and (π, π), respectively, and are given by

$$
\begin{aligned}
H_{int} = {} & u_1 \sum \alpha^\dagger_{i\mathbf{p}_3\sigma}\beta^\dagger_{j\mathbf{p}_4\sigma'}\beta_{j\mathbf{p}_2\sigma'}\alpha_{i\mathbf{p}_1\sigma} + u_2 \sum \beta^\dagger_{j\mathbf{p}_3\sigma}\alpha^\dagger_{i\mathbf{p}_4\sigma'}\beta_{j\mathbf{p}_2\sigma'}\alpha_{i\mathbf{p}_1\sigma} \\
& + \frac{u_3}{2} \sum \left[\beta^\dagger_{j\mathbf{p}_3\sigma}\beta^\dagger_{j\mathbf{p}_4\sigma'}\alpha_{i\mathbf{p}_2\sigma'}\alpha_{i\mathbf{p}_1\sigma} + h.c \right] + \frac{u_5}{2} \sum \left[\alpha^\dagger_{i\mathbf{p}_3\sigma}\alpha^\dagger_{i\mathbf{p}_4\sigma'}\alpha_{i\mathbf{p}_2\sigma'}\alpha_{i\mathbf{p}_1\sigma} + \beta^\dagger_{j\mathbf{p}_3\sigma}\beta^\dagger_{j\mathbf{p}_4\sigma'}\beta_{j\mathbf{p}_2\sigma'}\beta_{j\mathbf{p}_1\sigma} \right] \\
& + u_1^{(1)} \sum \beta^\dagger_{1\mathbf{p}_3\sigma}\beta^\dagger_{2\mathbf{p}_4\sigma'}\beta_{2\mathbf{p}_2\sigma'}\beta_{1\mathbf{p}_1\sigma} + u_2^{(1)} \sum \beta^\dagger_{2\mathbf{p}_3\sigma}\beta^\dagger_{1\mathbf{p}_4\sigma'}\beta_{2\mathbf{p}_2\sigma'}\beta_{1\mathbf{p}_1\sigma} \\
& + \frac{u_3^{(1)}}{2} \sum \left[\beta^\dagger_{2\mathbf{p}_3\sigma}\beta^\dagger_{2\mathbf{p}_4\sigma'}\beta_{1\mathbf{p}_2\sigma'}\beta_{1\mathbf{p}_1\sigma} + h.c. \right] + u_1^{(2)} \sum \alpha^\dagger_{1\mathbf{p}_3\sigma}\alpha^\dagger_{2\mathbf{p}_4\sigma'}\alpha_{2\mathbf{p}_2\sigma'}\alpha_{1\mathbf{p}_1\sigma} \\
& + u_2^{(2)} \sum \alpha^\dagger_{2\mathbf{p}_3\sigma}\alpha^\dagger_{1\mathbf{p}_4\sigma'}\alpha_{2\mathbf{p}_2\sigma'}\alpha_{1\mathbf{p}_1\sigma} + \frac{u_3^{(2)}}{2} \sum \left[\alpha^\dagger_{2\mathbf{p}_3\sigma}\alpha^\dagger_{2\mathbf{p}_4\sigma'}\alpha_{1\mathbf{p}_2\sigma'}\alpha_{1\mathbf{p}_1\sigma} + h.c. \right] \quad .
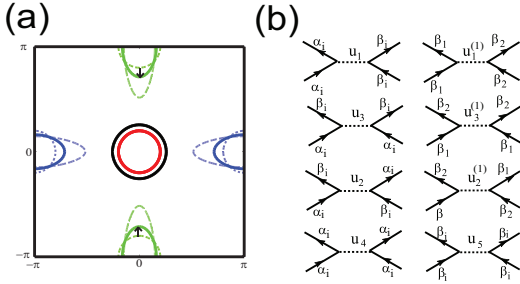\end{aligned}
\tag{2}
$$

FIG. 1: color online) (a) Calculated Fermi surfaces for the four band model. Solid and dashed lines for the electron FSs are for $\epsilon = 0.5$ and $\epsilon = 0.8$, respectively. The arrow shows the deviation from perfect nesting due to ellipticity; (b) Diagrammatic representations of the interactions in the four band model.

The vertices are shown diagrammatically in Fig. 1(b). For simplicity, we approximate all interactions as angle-independent, i.e., neglect the angle dependence introduced by dressing the interactions by coherence factors associated with the hybridization of Fe $d-$orbitals. These coherent factors do play a role for the structure of the SC gap[36], but do not substantially modify the spin resonance[20].

In the magnetically-disordered state transverse and longitudinal components of the spin susceptibility are undistinguishable, and we focus below on the transverse part. In the matrix RPA approximation, which we adopt, the transverse components of the full spin susceptibility $\chi^{i,j}$, where i and j are band indices, are related to transverse components of the bare susceptibility $\chi_0^{i,j}$ as

$$
\chi^{i,j} = \chi_0^{i,j} + \chi_0^{i,j'} u_{i',j'} \chi^{i',j} \quad . \tag{3}
$$

The summation over repeated band indices is assumed and $u^{i'j'}$ are matrix elements of the interactions shown in Fig.1(b) (contributions from all u^k are included in (3)).

The solution of Eq.(3) in matrix form is straightforward: $\hat{\chi} = \hat{\chi}_0(1 - \hat{u}\hat{\chi}_0)^{-1}$.

The components of the bare spin susceptibility $\hat{\chi}_0 = \chi_0^{i,j}(\mathbf{q}, i\Omega_m)$ are given by usual combinations of normal and anomalous Green's functions

$$
\begin{aligned}
\chi^{ij}(\mathbf{p}, i\Omega_m) = {} & -\frac{T}{2N} \sum_{\mathbf{k},\omega_n} \mathrm{Tr} \left[G^i(\mathbf{k}+\mathbf{p}, i\omega_n + i\Omega_m) G^j(\mathbf{k}, i\omega_n) \right. \\
& \left. + F^i(\mathbf{k}+\mathbf{p}, i\omega_n + i\Omega_m) F^j(\mathbf{k}, i\omega_n) \right]
\end{aligned}
\tag{4}
$$

where $G^i(\mathbf{k}, i\omega_n) = -\frac{i\omega_n + \varepsilon^i_{\mathbf{k}}}{\omega_n^2 + (\varepsilon^i_{\mathbf{k}})^2 + (\Delta^i_{\mathbf{k}})^2}$ and $F^i(\mathbf{k}, i\omega_n) = \frac{\Delta^i_{\mathbf{k}}}{\Omega_n^2 + (\varepsilon^i_{\mathbf{k}})^2 + (\Delta^i_{\mathbf{k}})^2}$.

The main contribution to the full spin susceptibility with momenta near $\mathbf{Q}$ comes from susceptibilities and interactions which involve hole and electron states (particle-hole bubbles made of one electron and one hole propagator, and u_1 and u_3 interaction terms in Eq. (2), see Ref. 10). For completeness, in numerical calculations we will keep all terms in the matrix equation for the full susceptibility. The results for the full $\sum_{ij} \chi^{ij}(\mathbf{p}, i\Omega_m)$ obtained this way do not differ much from those obtained by keeping only electron-hole bubbles and u_1 and u_3 interaction terms.

We do not present explicitly interactions leading to superconductivity and not discuss the solution of the pairing problem. This has been done in numerous other works on this subject[36]. We take the results of these studies as input and set the gap to be of $s^\pm$ type, with different sign between hole and electron pockets. More specifically, we set the gap to be a constant along the hole FSs, $\Delta^{\alpha_{1,2}} = \Delta_h$, and set the gap along the two electron FSs to be $\Delta^{\beta_{1,2}} = \Delta_e(1 \pm r\cos 2\phi)$, where ϕ is the angle counted from k_x direction in the UBZ. The gap $\Delta^{\beta_{1,2}}$ has no nodes if $r < 1$ and has accidental nodes when $r > 1$ at non-symmetry selected directions $\cos 2\phi = 1/r$. The numerical results presented below are obtained for $u_1 = u_3 \approx 0.25$eV (these numbers guarantee that system remains paramagnetic in the normal state),

and $u_5 = u_2 = 0.5u_1$, $u_i^{(j)} = 0.1u_i$. For simplicity we set $\Delta_h = -\Delta_e = \Delta$ although Δ_h and $-\Delta^{\beta_{1,2}}(\phi = \pi/4)$ do not have to be equal. For the gap we used $\Delta = 0.02t_\alpha$. For better convergence of numerical series we added a small damping $\Gamma = 1$meV to fermionic dispersion.

III. THE RESULTS

We present results systematically in three installations. We first consider the doping evolution of the resonance for a simple plus-minus gap and circular FSs, then we include the ellipticity of electron pockets, and finally we also include the angular dependence of the SC gap. For consistency with the experiments, we show all results in the folded BZ, when the commensurate resonance is at $\mathbf{Q} = (\pi, \pi)$.

A. Doping dependence of the resonance for plus-minus gap and circular FSs

This case is captured by setting $\epsilon = 0$ and $r = 0$ in $\Delta^{\beta_{1,2}}$. The doping dependence is parameterized by the change in the chemical potential $\delta\mu$.

Much in this case can be understood analytically. At zero doping, $\chi_0(\mathbf{Q}, \Omega)$ has a strong, square-root singularity at $\Omega = 2\Delta$. $Im\chi_0(\mathbf{Q}, \Omega)$ diverges as $1/\sqrt{\Omega - 2\Delta}$ at $\Omega > 2\Delta$ and $Re\chi_0(\mathbf{Q}, \Omega)$ diverges as $1/\sqrt{\Omega - 2\Delta}$ at $\Omega < 2\Delta$). For incommensurate momenta, $Im\chi_0(\mathbf{q}+\mathbf{Q}, \Omega)$ undergoes a finite jump at $\Omega = 2\Delta$ and $Re\chi_0(\mathbf{q} + \mathbf{Q}, 2\Delta)$ diverges logarithmically, as long as $q < 2k_F$. In this situation, the lowest Ω_{res} and the largest intensity are at the commensurate momentum $\mathbf{Q}$. We illustrate this in Fig. 2(a).

At a finite doping, $\chi_0(\mathbf{Q}, \Omega)$ still have a square-root singularity, but now the lower boundary of the particle-hole continuum shifts up and the singularity is located at a larger $\Omega_\mathbf{Q} = \sqrt{(2\Delta)^2 + (\delta\mu)^2}$. The resonance in the full $\chi(\mathbf{Q}, \Omega)$ is located below $\Omega_\mathbf{Q}$, but because $\Omega_\mathbf{Q}$ increases with $\delta\mu$, the position of the resonance at the commensurate $\mathbf{Q}$ also increases. Meanwhile, there exists the range of incommensurate momenta $\mathbf{q} + \mathbf{Q}$ for which the bottom of the particle-hole continuum is still located at $2\Delta_0$. These are $q_{min} < q < q_{max}$, where $q_{min} = \sqrt{k_F^2 + (\delta\mu)^2} - k_F$ and $q_{max} = \sqrt{k_F^2 + (\delta\mu)^2} + k_F$. For q inside this range, $Im\chi_0(\mathbf{q}+\mathbf{Q}, \Omega)$ undergoes a finite jump at $\Omega = 2\Delta$ and $Re\chi_0(\mathbf{q}+\mathbf{Q}, 2\Delta)$ diverges logarithmically, as before, but at the end points, i.e., at $q = q_{min}$ and $q = q_{max}$, hole and electron FSs touch each other after a shift by $\mathbf{Q}$, and $\chi_0(\mathbf{q} + \mathbf{Q}, \Omega)$ diverges by a power-law, this time as $1/(2\Delta - \Omega)^{1/4}$. Because of stronger divergence, the resonance in the full $\chi(\mathbf{q}+\mathbf{Q}, \Omega)$ at these q shifts down from 2Δ more than for other q, hence the dispersion of the resonance develops minima at $q = q_{min}$ and $q = q_{max}$.

At small doping, these two minima at incommensurate q are local minima because $\Omega_{res}(\mathbf{q} + \mathbf{Q})$ had an upward

dispersion around $\mathbf{Q}$ at zero doping, one needs some finite doping to change the sign of the slope at $q = 0$. As a result, at small but finite doping, the dispersion of the resonance has the global minimum at $q = 0$ and two roton-like minima at q_{min} and q_{max} (see Fig.2(b)). Once the doping gets larger, the resonance energy at $q = 0$ keeps going up together with the bottom of the particle-hole continuum, and eventually the global minimum of the resonance dispersion discontinuously shifts to a finite q, i.e., to an incommensurate momentum (see Fig.2(c)).
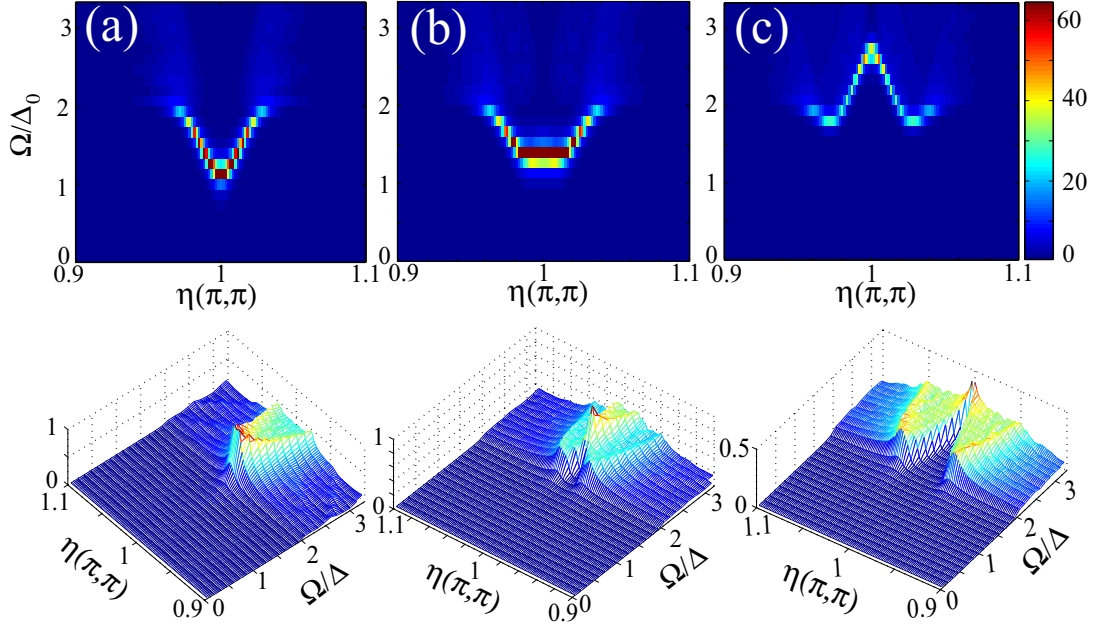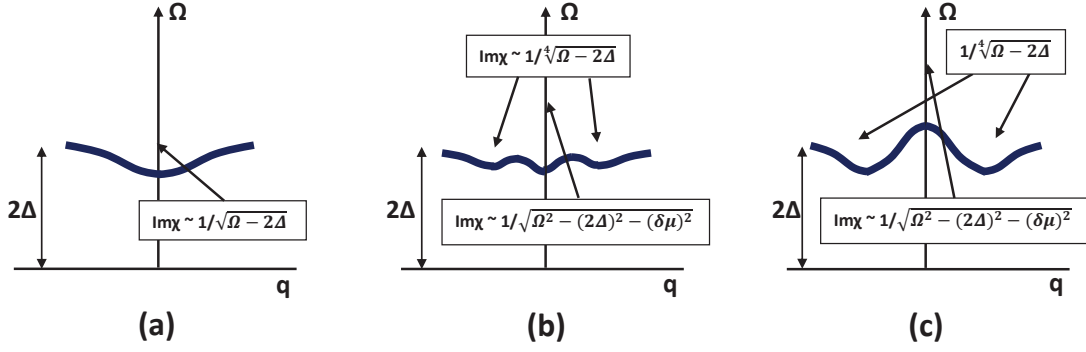
We reproduced this behavior in the numerical analysis. We display the numerical results in Fig. 3. The upper panels show the dispersion of the resonance energy, the lower panels show the imaginary part of $\chi_0(\mathbf{q} + \mathbf{Q}, \Omega)$. Fig.3(a) shows the behavior at zero doping. The 'square-root' divergence of $Im\chi_0(\mathbf{Q}, \Omega)$ at $\Omega = 2\Delta$ is clearly visible, while for nonzero $q < q_{max} = 2k_F$ we observe a 'jump' in $Im\chi_0(\mathbf{q} + \mathbf{Q}, \Omega)$ at $\Omega = 2\Delta$, in agreement with analytical consideration. We also see, at frequencies above 2Δ, the "upward" dispersion of the maximum in $Im\chi_0(\mathbf{q} + \mathbf{Q}, \Omega)$. This dispersion originates from the momentum dependence of the static $\chi_0(\mathbf{q}+\mathbf{Q})$ and gives rise to the upward dispersion of $\Omega_{res}(\mathbf{q}+\mathbf{Q})$ in the upper panel of Fig. 3(a).

In Figs. 3(b) we show the behavior of $Im\chi_0$ and the dispersion of the resonance at small but finite dopings $x = 0.01$ ($\delta\mu = -0.02$). We again see the square root singularity in $Im\chi_0(\mathbf{q} + \mathbf{Q}, \Omega)$ at the commensurate momentum $q = 0$, but now it shifts to a frequency above 2Δ, consistent with analytical $\Omega = \sqrt{(2\Delta)^2 + (\delta\mu)^2}$. We also clearly see additional singularity in $Im\chi_0(\mathbf{q} + \mathbf{Q}, \Omega)$ at an incommensurate momentum, which we associate with q_{min} (other momentum, g_{max} is outside the momentum range in 3 and $Im\chi_0(\mathbf{q} + \mathbf{Q}, \Omega)$ at such $\mathbf{q}$ already quite small). The resonance frequency $\Omega_{res}(\mathbf{q} + \mathbf{Q})$ still has a minimum at $\mathbf{q} = 0$, but because of an additional singularity in $Im\chi_0(\mathbf{q} + \mathbf{Q}, \Omega)$ at $\mathbf{q} = \mathbf{q}_{min}$, the dispersion of Ω_{res} around the minimum becomes rather flat. As doping is further increased to $x = 0.03$ ($\delta\mu = -0.051$) (Fig.3(c)), the square root singularity at $\mathbf{q} = 0$ is pushed further outward and $\Omega_{res}(\mathbf{Q})$ eventually moves to above 2Δ, while the one at $\mathbf{q} = \mathbf{q}_{min}$ stays below 2Δ. As a result, the minimum of Ω_{res} shifts from $\mathbf{q} = 0$ to $\mathbf{q} = \mathbf{q}_{min}$, as is clearly seen in the upper panel of Fig.3(c).

We found that the maximal intensity of the resonance does not immediately follow the position of the minimum of Ω_{res} and over some range of dopings is still the largest at the commensurate momentum $\mathbf{Q}$ even when the minimum of Ω_{res} already shifts to an incommensurate $\mathbf{q}+\mathbf{Q}$. But as doping increases even further, the maximum of the intensity eventually shifts to an incommensurate momentum.

B. Role of ellipticity of the electron pockets.

We next consider the case of elliptical electron pockets, when ϵ is nonzero. In this case, resonance may become

FIG. 2: (color online) Schematic form of the momentum dispersion of the spin resonance frequency Ω_{res} (solid line) at various doping and at zero ellipticity. Red dashed region is of the particle-hole continuum. The formulas show how the bare spin susceptibility diverges at the bottom of the continuum. Panel a – zero doping, panels (b),(c) – a finite doping (larger for c).

FIG. 3: (color online) The imaginary part of the total physical susceptibility $Im\chi(\mathbf{q} + \mathbf{Q}, \Omega)$ for various doping levels at zero ellipticity: (a) $x = 0$, (b)$x = 0.01(\delta\mu = -0.02)$, and (c)$x = 0.03(\delta\mu = -0.051)$. The lower panel shows the corresponding behavior of the imaginary part of the bare spin susceptibility.

incommensurate already at zero doping. Indeed, at $x = 0$ and non-zero ellipticity, Im $\chi_0(\mathbf{Q}, \Omega)$ has a finite jump at 2Δ because hole and electron velocities at each of the four hot spots (points where a hole pocket shifted by $\mathbf{Q}$ crosses an electron pocket) are neither parallel nor antiparallel. In other words, a square-root singularity at $\mathbf{Q}$ is cut by ϵ and is replaced by a jump. However, the power-law, $1/(2\Delta - \Omega)^{1/4}$, singularities at incommensurate q_{min} and q_{max} survive. Like before, $\mathbf{q}_{min}$ and $\mathbf{q}_{max}$ are the points where the hole FS, shifted by $\mathbf{Q}$, touches an elliptical electron FS. At the smaller $\mathbf{q} = \mathbf{q}_{min}$ four hot spots transform into two, at a larger $\mathbf{q} = \mathbf{q}_{max}$, the remaining two hot spots disappear. Because the shift of Ω_{res} from 2Δ is larger, the stronger is the divergence of Im $\chi_0(\mathbf{Q}, \Omega)$ at $\Omega = 2\Delta$, the minimum of the disper-

sion of Ω_{res} should eventually shift to an incommensurate momentum once ellipticity becomes large enough to overcome a positive curvature of the dispersion near $\mathbf{Q}$ which persists up to some finite ϵ. We found the same trends in the numerical calculations. In particular, in Fig.4 we show the evolution of the dispersion of the resonance and the form of $Im\chi_0(\mathbf{q} + \mathbf{Q}, \Omega)$ as a function of ellipticity at zero doping. We clearly see that once ϵ increases, the dispersion becomes more flat near the minimum at $\mathbf{Q}$, and eventually the minimum of the dispersion shifts to a non-zero $\mathbf{q}$, i.e., to an incommensurate momentum.

In Fig. 5 we combine finite doping and finite ellipticity. We see the same tends as before, namely at a given non-zero ϵ (we set $\epsilon = 0.3$ for definiteness), the resonance is quite broad already at $x = 0$ (Fig. 5(a)), it gets even
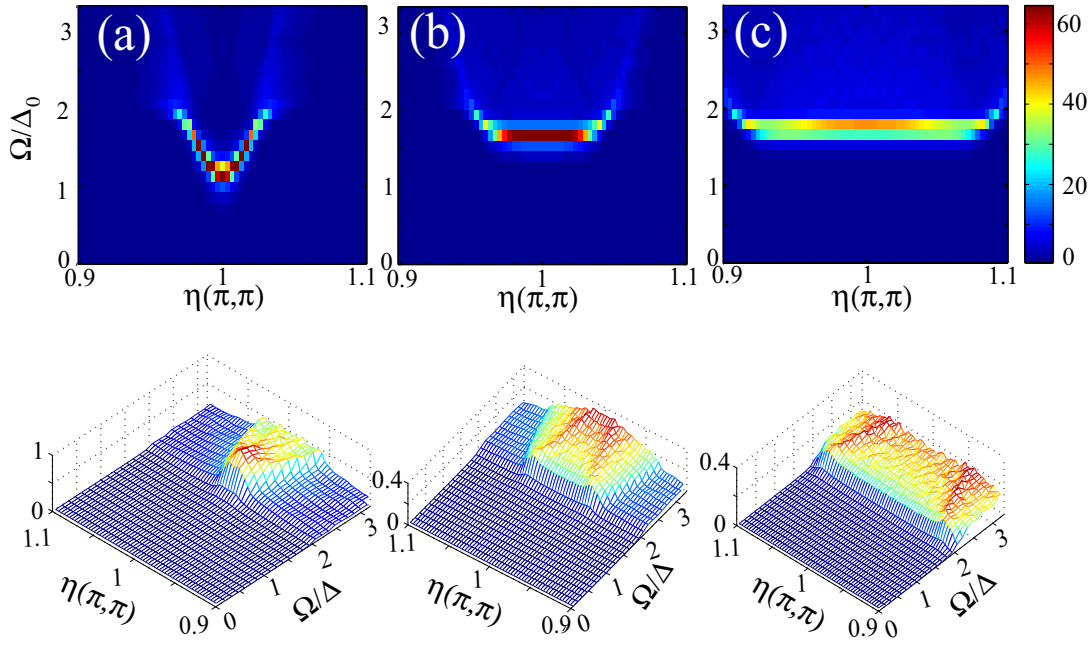
FIG. 4: (color online) The imaginary part of the total physical susceptibility $Im\chi(\mathbf{q} + \mathbf{Q}, \Omega)$ for various degrees of ellipticity at zero doping: (a) $\epsilon = 0.1$, (b) $\epsilon = 0.3$, and (c) $\epsilon = 0.5$. The lower panel shows the behavior of the imaginary part of the bare spin susceptibility.

more broad as x increases (Fig. 5(b)), and eventually incommensurate minima appear at large enough x (Fig. 5(c)). Note that at non-zero ellipticity the development of incommensurate minima in Ω_{res} at is less pronounced effect than at $\epsilon = 0$ and the key effect at small doping is the broadening of the resonance peak. This is because the bottom of the particle-hole continuum at $\mathbf{Q}$ does not move up with doping as long as an electron ellipses and a hole circle shifted by $\mathbf{Q}$ cross, and Ω_{res} at $\mathbf{Q}$ and at $\mathbf{q}+\mathbf{Q}$ with $q = q_{min}$ remain near-equal. Still, at larger dopings the resonance definitely becomes incommensurate, i.e., the minimum of Ω_{res} and the largest intensity shift to a incommensurate position $\mathbf{q} = \mathbf{q}_{min}$. There is another local minimum at $\mathbf{q} = \mathbf{q}_{max}$, like at $\epsilon = 0$, but that one corresponds to large enough $\mathbf{q}$ where $Im\chi_0$ is already small.

In all calculations presented so far we set $\Delta_h = -\Delta_e$. This was done chiefly to simplify the analytical calculations. Making the electron and hole gaps different in magnitude, but still with opposite signs, complicates the analysis does not change the results in any substantial way. For example Ω_Q, defined earlier in the text, changes from $\sqrt{(\delta\mu)^2 + (2\Delta)^2}$ to $\sqrt{(\delta\mu)^2 + (|\Delta_h| + |\Delta_e|)^2}$. Accordingly, the features, which happen at 2Δ for equal gaps, happen at $|\Delta_h| + |\Delta_e|$ for non-equal gaps, and the features at Δ (like those in density of states) become features at $min(\Delta_h, \Delta_e)$. As a result, the resonance is located at $\Omega < |\Delta_h| + |\Delta_e|$.

More substantial changes in the resonance occur once we include into consideration the fact that the electron gaps generally acquire angular dependence. This we dis-

cuss in the next subsection.

C. Role of the gap anisotropy

Another interesting aspect of the physics of the spin resonance in FeSCs is the role played by the angular dependence of the s^{+-}-wave gap. We remind that in FeSCs the gaps on the two electron FSs behave as $\Delta^{\beta_{1,2}} = -\Delta(1 \pm r \cos 2\phi)$, and r is generally a finite number. On general grounds we expect that the resonance gets broader simply because 2Δ becomes "soft" variable once the magnitude of 2Δ varies along the electron FS. Only at $T = 0$ and in the idealized case of no impurity scattering this "softness" does not matter because only fermions in the immediate vicinity of hot spots contribute to singularity in $Im\chi_0(\mathbf{q}+\mathbf{Q}, \Omega)$, and these fermions have some fixed Δ_k and Δ_{k+q+Q}. At a finite T and/or in the presence of some residual scattering, the momentum range for fermions contributing to the resonance increases and the angular dependence of the electron gap becomes relevant. Numerical calculations are in line with this reasoning. In Fig.6 (lower panel) we show the evolution with r of the bare susceptibility at $\mathbf{Q}$ taken between α_1 and β_1 bands. Other interband susceptibilities show qualitatively similar behavior. We set ellipticity and doping to be non-zero ($\epsilon = 0.5$, $x = 0.03$), so there is no power-law singularity at $\mathbf{Q}$. For $r = 0$, $Im\,\chi_0^{\alpha_1,\beta_1}(\mathbf{Q}, \Omega)$ then has a finite jump at 2Δ. We see that the jump persists also at a finite r, but its magnitude is reduced and the jump essentially disappears at $r > 1$. The reduction of
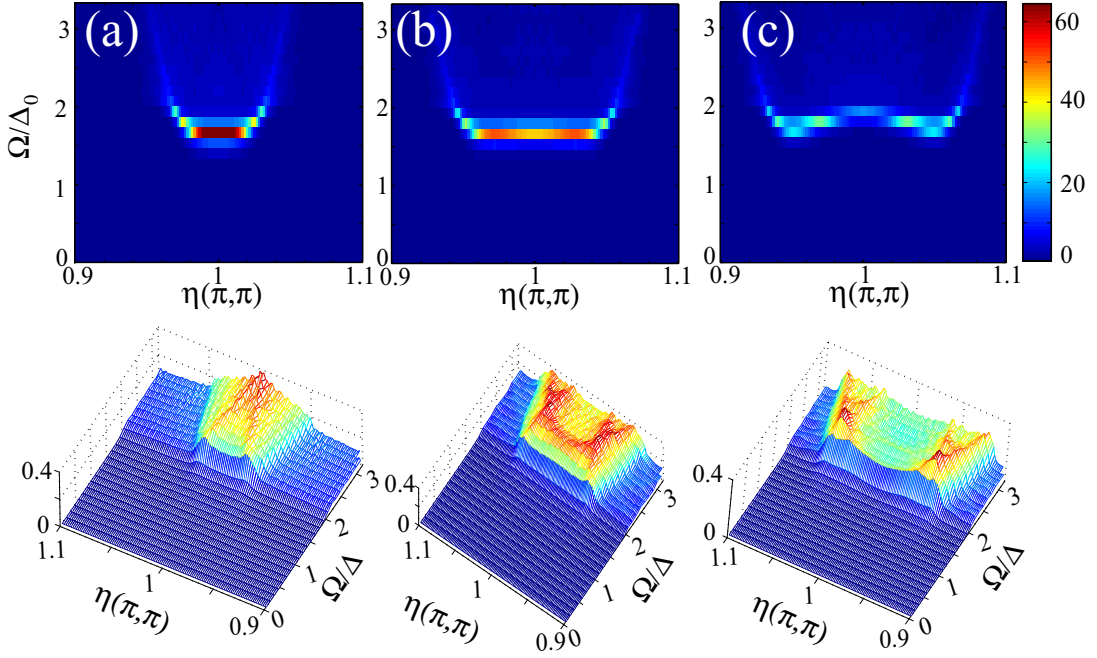
FIG. 5: (color online) The imaginary part of the total physical susceptibility $\mathrm{Im}\chi(\mathbf{q}+\mathbf{Q},\Omega)$ for various doping levels [(a) $x = 0(\delta\mu = 0)$, (b)$x = 0.02(\delta\mu = -0.035)$, and (c)$x = 0.05(\delta\mu = -0.076)$ and $\epsilon = 0.3$. The lower panel shows the corresponding behavior of the imaginary part of the bare spin susceptibility.

the jump affects the behavior of the full spin susceptibility, which we show in Fig. 6 (upper panel). We see that the resonance peak, which is already quite broad at $r = 0$, become even more broad at a finite r, and at large enough r the width of the resonance peak is essentially controlled by r.

The broadening of the peak at $\mathbf{Q}$ is wider than in the cuprates because there the FS is large and the momenta which contribute to the resonance are confined to near vicinity of hot spots, where Δ_k and $\Delta_{k+\mathbf{Q}}$ are rather flat and can be treated as constants[29]. In FeSCs, the FSs are much smaller and, accordingly, the effect of gap variation on the width of the resonance is stronger.

Strong enhancement of the width of the resonance peak due to angle variation of the SC gap is the possible explanation why the observed peak at $\mathbf{Q}$ is wider than one should expect from the fully gapped $s^{\pm}$-state[18]. Another possible explanation is the effect of impurities, which we consider in the next section.

The effect of the gap variation on the dispersion of the resonance is strongest at $\mathbf{Q}$ because for incommensurate momenta and, particularly, for $q = q_{min}$, the gaps on hole and electron FSs differ quite substantially by magnitude, and, when $r > 1$, have the same sign. A simple reasoning shows that, in this situation, two effects happen: the bottom of the particle-hole continuum goes down near $\mathbf{q}_{min}$, and, at the same time, the intensity of the resonance peak at $\mathbf{q}_{min}$ drops, and for $r > 1$ the resonance at $\mathbf{q} \sim q_{min}$ simply does not exist. The outcome is that, as r increases, the resonance dispersion flattens up near $\mathbf{Q}$ and the intensity drops away from $\mathbf{Q}$. As shown in Fig.6

the numerical analysis is again in line with this reasoning.

D. $s^{\pm}$ versus s^{++}-wave gap

For completeness, we also briefly address the issue of the interplay between spin response in superconductors with $s^{\pm}$ and s^{++} gaps in a situation when the original and the shadow FSs do not cross, which is the case when both hole and electron FSs are near-circular and the doping is finite, such that one FS is larger than the other. The case when the original FSs cross is quite similar to the cuprates, and the absence of spin resonance for s^{++} gap in this situation has been discussed earlier[29].

We show that there is no resonant enhancement of the $\mathrm{Im}\chi$ for the s^{++}-wave case even when the original and the shadow FSs do not cross. To do so we look into the case with no impurity scattering and no ellipticity and compute

$$\chi_0^{\alpha\beta}(Q, i\Omega) = -N_0 T \sum_n \int d\varepsilon G^{\alpha}(i\omega_n, \varepsilon) G^{\beta}(i\omega_n + \Omega, \varepsilon + \delta\mu)$$

$$(5)$$

where $\delta\mu$ is proportional to the mismatch in FS radii due to doping. And α and β refer to the hole and electron FSs respectively. In the absence of impurities we return to the case where $\bar{\Delta}_\omega$ is frequency independent and simply equal to Δ. In the normal state we get

$$\mathrm{Im}\chi_0(Q, \Omega) = N_0 \frac{\pi^2}{2}\theta(\Omega - |\delta\mu|) \quad (6)$$

9

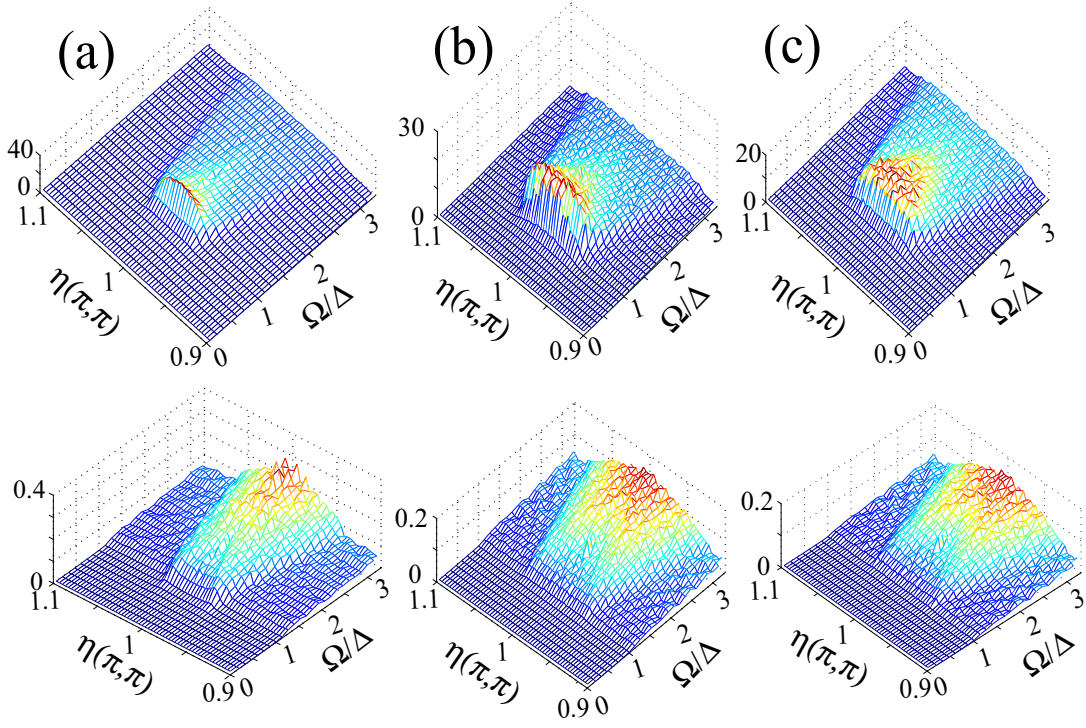FIG. 6: (color online) The imaginary part of the bare interband susceptibility $Im\chi^{\alpha_1\beta_1}(\mathbf{Q},\omega)$(lower panel) and the total physical susceptibility (upper panel) for (a)$r=0.5$, (b)$r=1$, and (c)$r=2$. We set $x=0.03$ and $\epsilon=0.5$.

In the SC state (after appropriately adding the F*F term), we get

$$Im\chi_0(Q,\Omega) = -N_0\frac{\pi^2}{4}\sum_x \frac{\Delta(\Delta+\Delta_Q)+(\omega+x)(\Omega-\delta\mu)}{|\Omega x - \delta\mu\,\omega|} \tag{7}$$

where Δ and Δ_Q are the gaps on the hole and electron FSs, and the two values of x which are summed over are given by

$$x = -\frac{\delta\mu}{2} \pm \frac{\Omega}{2}\sqrt{\frac{\left(\frac{\Omega}{2}\right)^2 - \left(\frac{\delta\mu}{2}\right)^2 - \Delta^2}{\left(\frac{\Omega}{2}\right)^2 - \left(\frac{\delta\mu}{2}\right)^2}} \tag{8}$$

For zero doping ($\delta\mu=0$), for $s^\pm$ SC, $\Delta = -\Delta_Q$ and we have

$$Im\chi_0^{s^\pm} = N_0\frac{\pi^2}{2}\frac{1}{\sqrt{1-\left(\frac{2\Delta}{\Omega}\right)^2}} \tag{9}$$

This implies that $Re\chi_0$ has a square-root singularity at $\Omega=2\Delta$ and hence the full $Im\chi^{s^\pm}(\mathbf{Q},\Omega)$ has a pole (resonance) at some $\Omega < 2\Delta$.

For s^{++} case $\Delta=\Delta_Q$, and we get

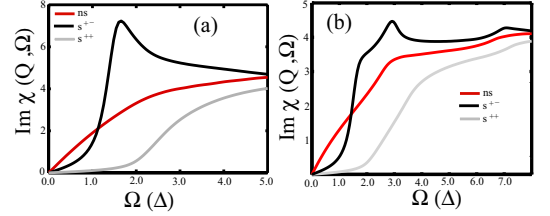$$Im\chi_0^{s^{++}} = N_0\frac{\pi^2}{2}\sqrt{1-\left(\frac{2\Delta}{\Omega}\right)^2} \tag{10}$$

FIG. 7: (color online) Calculated frequency dependence of the imaginary part of the total physical susceptibility for (a)$\epsilon=0.3$ and (b)$\epsilon=0$ for the s^{++}-wave superconductor. We set $x=0.01$ ($\delta\mu=-0.02$). We clearly see that there is no resonant enhancement of the full spin susceptibility for s^{++} gap. To soften $\delta-$function in the $s^\pm$ case we averaged $Im\chi(\mathbf{Q},\Omega)$ around $\mathbf{Q}$ with $\delta\mathbf{q}=\pm0.1\mathbf{Q}$

As expected, there is no jump in $Im\chi_0^{s^{++}}(\mathbf{Q},\Omega)$ at 2Δ implying no singularity in $Re\chi_0$ and hence no resonance in $Im\chi^{s^{++}}(\mathbf{Q},\Omega)$ below $\Omega=2\Delta$.

Consider next the case when $\delta\mu$ is non-zero. Now $Im\chi_0(Q,\Omega)$ has a singularity at $\Omega=\sqrt{(\delta\mu)^2+4\Delta^2}$. Expanding around this Ω by introducing a small z such that $\left(\frac{\Omega}{2}\right)^2 = \left(\frac{\delta\mu}{2}\right)^2 + \Delta^2 + z^2$, we find using Eq. 7, that

$$Im\chi_0^{s^\pm}(z) = N_0\frac{\pi^2}{2}\frac{\Delta}{z} \tag{11}$$

and

$$Im\chi_0^{s++}(z) = N_0 \frac{\pi^2}{2} z \qquad (12)$$

So the main result is the same as with no doping – Im $\chi_0^{s\pm}(z)$ is singular at $z = 0$, the singularity in Im $\chi_0^{s\pm}(0)$ gives rise to the singularity in Re $\chi_0^{s++}(0)$ and to resonance at a smaller frequency. On the other hand, Im $\chi_0^{s++}(z)$ is non-analytic at $z = 0$, but not singular, hence Re $\chi_0^{s++}(0)$ is also not singular, and Im $\chi_0^{s++}(z)$ remains non-singular below the bottom of the particle-hole continuum. We further confirm these statements by performing the numerical calculations for our four-band model. We show the results in Fig.7.

IV.   EFFECT OF IMPURITIES

In this section we study how the position and the width of spin resonance are affected by elastic impurity scattering. We consider both magnetic and non-magnetic impurities. To keep the calculations tractable we make several simplifying assumptions: (i) we only consider resonance

at $T = 0$ and at the commensurate momentum $\mathbf{Q}$, (ii) we neglect ellipticity of electron pockets and the angle variation of the SC gap, and (iii) we approximate the band dispersion by the two-band model of one hole and one electron pockets (α- and β-fermions) separated by $\mathbf{Q} = (\pi, \pi)$ and perfectly nested, i.e., set $\varepsilon^\alpha(\mathbf{k}) = -\varepsilon^\beta(\mathbf{k} + \mathbf{Q})$ and, in the absence of impurities, $\Delta^\alpha = -\Delta^\beta = \Delta$. We show that impurity scattering broadens the resonance but its energy position $\Omega_{res}(\mathbf{Q})$ can remain essentially intact. Because T_c for $s^\pm$ pairing drops with impurity scattering, the ratio Ω_{res}/T_c increases, in agreement with the experimental data. Because both the broadening of the resonance and the increase of Ω_{res}/T_c with impurity scattering are related to $s^\pm$ gap symmetry, we expect that these two results survive for more realistic 4-5 band models with elliptical electron FSs and angle-dependent gap.

A.   Method

Non-magnetic impurities affect electrons via the impurity scattering potential in the form

$$H_{imp} = \sum_{\mathbf{k_1,2}} \left[U_0(\mathbf{k_1} - \mathbf{k_2}) \left(\alpha_{\mathbf{k_1}\sigma}^\dagger \delta_{\sigma\sigma'} \alpha_{\mathbf{k_2}\sigma'} + \beta_{\mathbf{k_1}\sigma}^\dagger \delta_{\sigma\sigma'} \beta_{\mathbf{k_2}\sigma} \right) + U_\pi(\mathbf{k_1} - \mathbf{k_2}) \left(\alpha_{\mathbf{k_1}\sigma}^\dagger \delta_{\sigma\sigma'} \beta_{\mathbf{k_2}\sigma'} + \beta_{\mathbf{k_1}\sigma}^\dagger \delta_{\sigma\sigma'} \alpha_{\mathbf{k_2}\sigma'} \right) \right] \quad (13)$$

where $U_0(\mathbf{k_1} - \mathbf{k_2})$ and $U_\pi(\mathbf{k_1} - \mathbf{k_2})$ are intra- and inter-band scattering terms, respectively. For U_0, $\mathbf{k_1}$ and $\mathbf{k_2}$ are both near $(0,0)$ or $\mathbf{Q}$, while for U_π $\mathbf{k_1} \approx (\mathbf{0,0})$ and $\mathbf{k_2} \approx \mathbf{Q}$ or vice versa. Quite generally one expects $U_\pi <$

U_0 for any impurity potential with a finite range in real space.

Paramagnetic impurities in turn affect electrons via the spin-dependent potential

$$H_{p\,mag} = \sum_{\mathbf{k_1,2}} U_0^p(\mathbf{k_1} - \mathbf{k_2}) \left(\alpha_{\mathbf{k_1}\sigma}^\dagger \vec{\sigma}_{\sigma\sigma'} \cdot \vec{S} \alpha_{\mathbf{k_2}\beta} + \beta_{\mathbf{k_1}\sigma}^\dagger \vec{\sigma}_{\sigma\sigma'} \cdot \vec{S} \beta_{\mathbf{k_2}\beta} \right) +$$

$$U_\pi^p(\mathbf{k_1} - \mathbf{k_2}) \left(\alpha_{\mathbf{k_1}\sigma}^\dagger \vec{\sigma}_{\sigma\sigma'} \cdot \vec{S} \beta_{\mathbf{k_2}\sigma'} + \beta_{\mathbf{k_1}\sigma}^\dagger \vec{\sigma}_{\sigma\sigma'} \cdot \vec{S} \alpha_{\mathbf{k_2}\sigma'} \right) \qquad (14)$$

where $\vec{\sigma} = (\sigma_x, \sigma_y, \sigma_z)$ and σ_i are Pauli matrices, and $\vec{S}$ is the static impurity spin with the property $< S_i S_j >_{impurity\ sites} = \frac{S(S+1)}{3} \delta_{i,j}, i, j \in \{x, y, z\}$.

yields

Fermionic propagators for an $s^\pm$ superconductors in the presence of non-magnetic impurities have been considered before (see e.g., Ref. 10). The extension to include paramagnetic impurities is straightforward, and

$$G^{\alpha,\beta} = -\frac{Z\,i\omega_m + \varepsilon_{\mathbf{k}}^{\alpha,\beta}}{Z^2(\omega_m^2 + |\bar{\Delta}_\omega|^2) + (\varepsilon_{\mathbf{k}}^{\alpha,\beta})^2}$$

$$F^{\alpha,\beta} = \pm\frac{Z\bar{\Delta}_\omega}{Z^2(\omega_m^2 + |\bar{\Delta}_\omega|^2) + (\varepsilon_{\mathbf{k}}^{\alpha,\beta})^2} \qquad (15)$$

with

$$Z = 1 + \frac{u_0 + u_\pi + u_0^p + u_\pi^p}{\sqrt{\omega_m^2 + |\bar{\Delta}_\omega|^2}}$$

$$\left(\frac{\bar{\Delta}_\omega}{\Delta_b} - 1\right)^2 = b^2 \frac{\bar{\Delta}_\omega^2}{\omega_m^2 + |\bar{\Delta}_\omega|^2}$$

$$b = \frac{2(u_\pi + u_0^p)}{\Delta_b}. \qquad (16)$$

where we have adopted, for brevity, the notation $u_0 \equiv n_{imp}|U_0(0)|^2$ (and a similar for u_π, u_0^p, and u_π^p), with n_{imp} being the impurity concentration. In Eq. (16), $\bar{\Delta}_\omega$ is the actual, frequency-dependent gap in the presence of impurity scattering, and Δ_b is the order parameter related to $\bar{\Delta}_\omega$ via

$$\frac{\Delta_b}{\Delta_0} = \frac{\int_0^{\omega_{max}} d\omega_m \frac{\bar{\Delta}_\omega}{|\bar{\Delta}_\omega|^2 + \omega_m^2}}{\int_0^{\omega_{max}} d\omega_m \frac{\Delta_0}{\Delta_0^2 + \omega_m^2}} \qquad (17)$$

For any $b \neq 0$, a non-zero fermionic DOS $N(\omega) = (m/2\pi)Re\left[\omega/\sqrt{\omega^2 - \bar{\Delta}_\omega^2}\right]$ extends to frequencies below 2Δ. For $0 < b < 1$, the system still preserves the gap in the fermionic DOS near zero frequency, i.e., over some range of ω near $\omega = 0$, $N(\omega) = 0$. For $b > 1$, the system enters into a gapless regime, in which $\bar{\Delta}_\omega$ scales as

$i\omega$ at the lowest frequencies and $N(\omega = 0)$ is non-zero, although reduced compared to the DOS in the normal state.

Observe that the gap renormalization comes from interband non-magnetic impurity scattering and intraband magnetic impurity scattering which are pair-breaking for $s^\pm$ superconductor (both also reduce T_c). At the same time intraband non-magnetic impurity scattering and interband magnetic impurity scattering do not contribute to b and therefore are not pair-breaking. If only these two scattering were present, b would be zero, $\bar{\Delta}_\omega$ would be equal to Δ, and Eq. (17) would then yield $\bar{\Delta}_\omega = \Delta_b = \Delta$, i.e., the gap would not be affected by impurities. The same analysis extended to a finite T shows that u_0 and u_π^p also do not affect T_c.

The next step is to use normal and anomalous Green's functions from (15) and compute spin susceptibility for a dirty BCS superconductor. This has to be done with care, though, as one has to include not only self-energy corrections, incorporated in (15), but also series of vertex corrections which are of the same order as self-energy terms. We follow the treatment by Gorkov and Rusinov[37], sum up ladder series of vertex correction diagrams and after straightforward algebra obtain

$$\chi_0(\mathbf{Q}, \Omega) = N_0 \int \frac{d\omega}{2\pi} F_{\Delta^2} \left[\frac{1}{1 + (u_0 + u_\pi - \frac{1}{3}(u_0^p + u_\pi^p))F_{\Delta^2} + (u_0 - u_\pi + \frac{1}{3}(u_0^p - u_\pi^p))\frac{F_{\omega\Delta}^2}{F_{\Delta^2}}} \right]. \qquad (18)$$

where N_0 is the 2D density of states, and

$$F_{\Delta^2} = \frac{-\omega(\omega + \Omega) + \bar{\Delta}_\omega \bar{\Delta}_{\omega+\Omega} + f_\omega f_{\omega+\Omega}}{f_\omega f_{\omega+\Omega}(f_\omega + f_{\omega+\Omega} + 2u_0 + 2u_\pi)} \qquad (19)$$

$$F_{\omega\Delta} = \frac{\omega \bar{\Delta}_{\omega+\Omega} - (\omega + \Omega)\bar{\Delta}_\omega}{f_\omega f_{\omega+\Omega}(f_\omega + f_{\omega+\Omega} + 2u_0 + 2u_\pi)} \qquad (20)$$

with $f_\omega = \sqrt{\bar{\Delta}_\omega^2 - \omega^2}$.

As before, we assume that the full susceptibility $\chi(\mathbf{Q}, \Omega)$ is related to $\chi_0(\mathbf{Q}, \Omega)$ as $\chi(\mathbf{Q}, \Omega) = \chi_0(\mathbf{Q}, \Omega)/(1 - u_{spin}\chi_0(\mathbf{Q}, \Omega))$. Where u_{spin} is the residual interaction in the spin channel (see SecII).

We solved for $\bar{\Delta}_\omega$, substituted the result into (18), integrated over frequency and obtained bare $\chi_0(\mathbf{Q}, \Omega)$ and the full Im $\chi(\mathbf{Q}, \Omega)$ as functions of impurity scattering.

B. Results

We first discuss the role of non-magnetic impurities u_0 and u_π and for this purpose set u_0^p and u_π^p to zero in Eq.

(16). Both u_0 and u_π renormalize quasiparticle Z, but only u_π contributes to pair-breaking parameter b.

In Fig.8(a)-(b) we show the calculated Im$\chi(\Omega)$ for various values of b and for two different u_0. Im$\chi(\Omega)$ for $b = 0$ is shown in panel (c) for comparison. We see that for $b \sim 0.3 - 0.6$ used earlier to fit NMR, penetration depth and uniform spin susceptibility data (see Refs. 10,38) the resonance peak in Im$\chi(\mathbf{Q}, \Omega)$ falls into the frequency range where the spin response in a dirty $s^\pm$ SC is no longer a δ-function, and its width increases with increasing b. At the same time, the position of the resonance remains almost intact. Despite that Δ_b and T_c obviously decrease when b increases. To emphasize this point we plot in Fig.9 Ω_{res} as a function of b together with $T_c(b)$ calculated from the conventional relation[38]

$$\ln\left(\frac{T_c}{T_{c_0}}\right) = \psi\left(\frac{1}{2}\right) - \psi\left(\frac{1}{2} + \frac{b\Delta}{2\pi T_c}\right), \qquad (21)$$

where ψ is the digamma-function and T_{c0} is the transition temperature in the clean limit. We clearly see that T_c decreases with b while Ω_{res} remains practically unchanged, such that the experimentally measured ratio
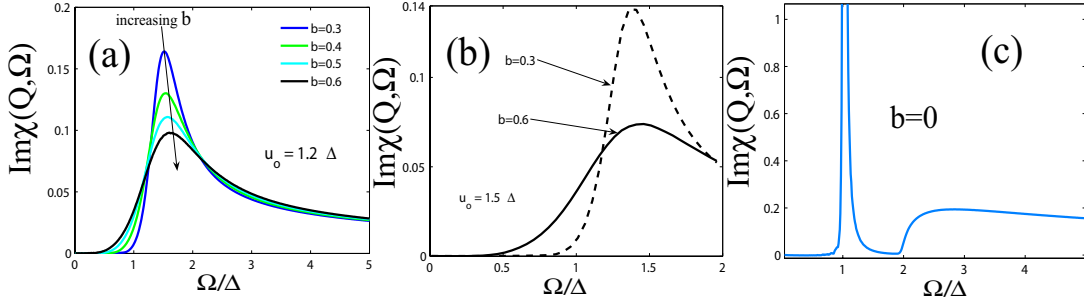
FIG. 8: Calculated $\mathrm{Im}\chi(\mathbf{Q},\Omega)$ for scattering by non-magnetic impurities, for different values of b, which scales with the strength of the interband impurity scattering. We used $u_0 = 1.2\Delta$ (a) and $u_0 = 1.5\Delta$ (b). Figure (c) shows, for comparison, the resonance peak for $b = 0$.
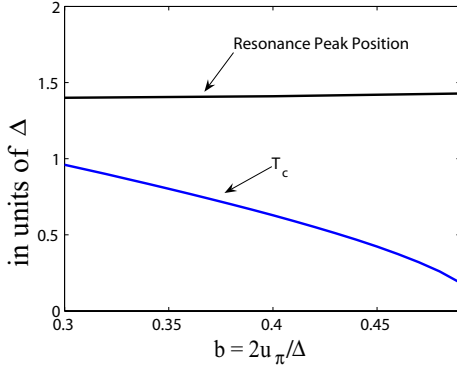

FIG. 9: Scattering by non-magnetic impurities. Evolution of T_c and the resonance peak position (both in units of Δ) as a function of b.
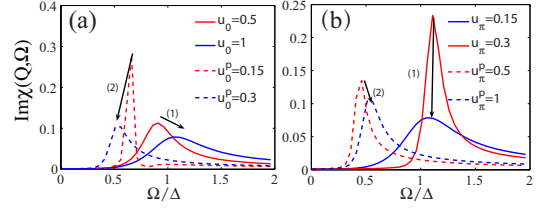

FIG. 10: The effect of (a) intra-band and (b) inter-band impurity scattering on the resonance peak in iron-based superconductors. In particular, (a) shows the influence of the increasing intra-band non-magnetic and magnetic scattering potential, while (b) displays the corresponding effect of the inter-band impurity scattering. In both cases, the solid and dashed curves refer to the non-magnetic and magnetic impurity scattering, respectively. While studying the effect of magnetic impurities, we kept the non-magnetic impurities as constants and vice versa.

Ω_{res}/T_c increases with the strength of intra-band impurity scattering. This trend is consistent with the observed doping dependence of Ω_{res}/T_c in $\mathrm{Ba}_{1-x}\mathrm{K}_x\mathrm{Fe}_2\mathrm{As}_2$ above optimal doping, where the decrease of T_c with increasing K concentration is believed to be at least partly due to increased impurity scattering[39].

We next keep u_0^p and u_π^p non zero and compare the effects of non-magnetic and magnetic impurities.

In Fig.10(a) we show how the resonance profile evolve once we increase small momentum impurity-scattering terms u_0 and u_0^p. We see that in both cases the peak broadens but it is shifted in opposite directions – upwards when u_0 increases and downwards when u_0^p increases. Also, the broadening is much stronger under the change of u_0^p. Fig.10(b) shows the effect on the peak of magnetic and non-magnetic inter-band scattering u_π and u_π^p. We see that the increase of u^π strongly broadens the peak and weakly shifts it downwards, while the increase of $u^p\pi$ has weaker effect on the width of the peak and shifts its position slightly upwards. This behavior is expected because, like we said, in an $s^\pm$-wave superconductor the interband non-magnetic impurity scattering u_π behaves much like a magnetic intra-band scattering, u_0^p. Therefore u_π and u_0^p should give rise to qualitatively similar effects on the resonance peak. This is indeed what

we have found (compare arrow (2) in Fig. 10(a) and arrow (1) in Fig.10(b)). Likewise, the interband magnetic scattering, u_π^p and the intraband non-magnetic scattering u_0 should have similar effect on the resonance, and this also agrees with Fig. 10 (compare arrow (1) in Fig. 10(a) and arrow (2) in Fig.10(b)). One has to bear in mind, however, that the effects of u_π and u_0^p and of u_0 and u_π^p are similar but not equivalent because vertex corrections behave differently for magnetic and non-magnetic impurity scatterings (see Eq.(18)), independent on whether this is intra- or inter-band scattering. Still, the results in Fig. 10 clearly show that pair-breaking u_π and u_0^p have the strongest effect on the resonance peak. Both impurity scatterings broaden the peak but only slightly affect its position such that Ω_{res}/T_c increases when the concentration of either non-magnetic or magnetic impurities increases. This is the key result of this section.

V. CONCLUDING REMARKS

In this work we have shown that the intensity and position of the resonance peak depends on several factors: doping, ellipticity of the electron pockets; gap anisotropy

and the presence accidental nodes on the electron pockets, and magnetic and non-magnetic impurity scattering.

We find that with no ellipticity, the resonance starts at the commensurate momentum below 2Δ and moves outward in energy with doping. At some doping, the minimum in the dispersion of the resonance jumps to an incommensurate momentum, and at even larger doping the intensity of the resonance becomes the largest at the incommensurate momentum. With finite ellipticity, the intensity becomes the largest at the incommensurate momenta at smaller dopings, and for large enough ellipticity the resonance becomes incommensurate already at zero doping. Besides, at finite ellipticity, the resonance peak gets quite broad The inclusion of the angular variation of the $s^{\pm}-$ leads to further broadening of the resonance peak, particularly when the gap has accidental nodes on the electron pockets. The broadening of the resonance may actually be even stronger than in $d-$wave cuprate superconductors.

We further analyzed the sensitivity of the resonance to non-magnetic as well as magnetic impurities. We obtain that both non-magnetic and magnetic impurities have pair-breaking components which broaden the resonance but do not shift much its position compared to the clean case. The reduction of T_c by the same impurity scattering is much stronger, such that the ratio $\Omega_{res}/\mathrm{T}_c$ increases with the strength of impurity scattering.

Finally we found that a true resonance is only possible for an $s^{\pm}$ gap and does not occur if the gap has s^{++} structure, even when the original and shadow FS do not cross each other.

The transformation of the minimum in the dispersion of the resonance and the maximum of its intensity from the commensurate to the incommensurate momentum upon doping is consistent with recent study of the doping evolution of the resonance in the hole-doped compound $\mathrm{Ba}_{1-x}\mathrm{K}_x\mathrm{Fe}_2\mathrm{As}_2$[30]. The same study also found that Ω_{res}/T_c increases with doping, particularly in overdoped $\mathrm{Ba}_{1-x}\mathrm{K}_x\mathrm{Fe}_2\mathrm{As}_2$, where the decrease of T_c with doping can at least partly be attributed to impurities. The increase of Ω_{res}/T_c with increasing impurity scattering is consistent with our theory.

The situation in electron-doped materials is less certain. From theory perspective, the resonance peak must become incommensurate at large enough electron doping. The transformation from a commensurate to an incommensurate static antiferromagnetic order has been observed in the normal state measurements of electron-doped $\mathrm{Ba}(\mathrm{Fe}_{1-x}\mathrm{Co}_x)_2\mathrm{As}_2$ at $x > 0.056$ (Ref. 40). We, however, not aware of the experimental observation of the incommensurate resonance peak in the superconducting state of electron-doped materials. Possible reasons may be quasiparticle damping and substantial ellipticity of the electron pockets which make the transformation from commensurate to incommensurate resonance in a superconductor much less visible than for a circular FSs (see Figs. 3 and 4). We note in this regard that in the hole doped $\mathrm{Ba}_{1-x}\mathrm{K}_x\mathrm{Fe}_2\mathrm{As}_2$ the splitting from a commensurate to an incommensurate resonance is clearly resolved only around $x \sim 0.5$.[30] At this range of electron (Co) doping the material is no longer a superconductor.

[1] see e.g., M. Eschrig, Adv. Phys. **55**, 47 (2006) and references therein to early works on the resonance.

[2] E. Demler and S.C. Zhang, Phys. Rev. Lett. **75**, 4126 (1995); E. Demler, H. Kondo, and S.C. Zhang, Phys. Rev. B **58**, 5719 (1998); O. Tchernyshyov, M. R. Norman, and A. V. Chubukov, Phys. Rev. B **63**, 144507 (2001); W.C. Lee et al, Phys. Rev. B 77, 214518 (2008) W.C. Lee and A.H. MacDonald, Phys. Rev. B **78**, 174506 (2008).

[3] Z. Hao and A. V. Chubukov Phys. Rev. B **79**, 224513 (2009).

[4] A. V. Chubukov and L.P. Gorkov, Phys. Rev. Lett. **101**, 147004 (2008).

[5] A. J. Millis and H. Monien, Phys. Rev. B **54**, 16172 (1996).

[6] J. Rossat-Mignod, L.P. Regnault, C. Vettier, P. Bourges, P. Burlet, J. Bossy, J.Y. Henry, G. Lapertot, Physica C **185-189**, 86 (1991); H. Mook, M. Yethiraj, G. Aeppli, T. E. Mason, T. Armstrong, Phys. Rev. Lett. **70**, 3490 (1993); H.F. Fong, P. Bourges , Y. Sidis, L.P. Regnault, A. Ivanov, G.D. Gu, N. Koshizuka, B. Keimer, Nature **398**, 588 (1999); Ph. Bourges, Y. Sidis, H.F. Fong, L.P. Regnault, J. Bossy, A. Ivanov, B. Keimer, Science **288**, 1234 (2000), H. He, P. Bourges, Y. Sidis, C. Ulrich, L. P. Regnault, S. Pailhes, N.S. Berzigiarova, N.N. Kolesnikov, B. Keimer, Science **295**, 1045 (2002).

[7] N.K. Sato, N. Aso, K. Miyake, R. Shiina, P. Thalmeier, G. Varelogiannis, C. Geibel, F. Steglich, P. Fulde, and T. Komatsubara, Nature **410**, 340 (2001).

[8] C. Stock, C. Broholm, J. Hudis, H.J. Kang, and C. Petrovic, Phys. Rev. Lett. **100**, 087001 (2008).

[9] I.I. Mazin, arXiv:1102.3655 (unpublished).

[10] A. V. Chubukov, D. V. Efremov, and I. Eremin, Phys. Rev. B **78**, 134512 (2008); A. V. Chubukov, Physica C **469**, 640 (2009); A. V. Chubukov, M. G. Vavilov, and A. B. Vorontsov, Phys. Rev. B **80**, 140515 (2009).

[11] I.I. Mazin, D.J. Singh, M.D. Johannes, and M.H. Du, Phys. Rev. Lett. **101**, 057003 (2008).

[12] S. Graser, T. A. Maier, P. J. Hirschfeld, D. J. Scalapino, New J. Phys. **11**, 025016 (2009); T.A. Maier, S. Graser, D.J. Scalapino, P.J. Hirschfeld, Phys. Rev. B 79, 224510 (2009).

[13] V. Cvetkovic and Z. Tesanovic, EPL **85**, 37002 (2009); V. Stanev, J. Kang, and Z. Tesanovic, Phys. Rev. B 78, 184509 (2008).

[14] Fa Wang, Hui Zhai, Ying Ran, Ashvin Vishwanath, and Dung-Hai Lee, Phys. Rev. Lett., 102, 047005 (2009); Fa Wang, Hui Zhai, and Dung-Hai Lee, Phys. Rev. B **81**, 184512 (2010);

[15] R. Thomale, Ch. Platt, J. Hu, C. Honerkamp, and B.A. Bernevig, Phys. Rev. B **80**, 180505(R) (2009); R. Thomale, Ch. Platt, W. Hanke, B.A. Bernevig, Phys. Rev. Lett. **106**, 187003 (2011).

[16] K. Kuroki, S. Onari, R. Arita, H. Usui, Y. Tanaka, H. Kontani, and H. Aoki, Phys. Rev. Lett. **101**, 087004 (2008); K. Kuroki, H. Usui, S. Onari, R. Arita, and H. Aoki, Phys. Rev. B **79**, 224511 (2009).

[17] V. Barzykin and L. P. Gorkov, Pis'ma v ZhETF **88**, 142 (2008) [JETP Lett. **88**, 131 (2008)].

[18] H. Kontani and S. Onari, Phys. Rev. Lett. **104**, 157001 (2010).

[19] M.M. Korshunov, and I. Eremin, Phys. Rev. B **78**, 140509(R) (2008).

[20] T. A. Maier, S. Graser, D. J. Scalapino, and P. Hirschfeld, Phys. Rev. B **79**, 134520 (2009); T.A. Maier, and D.J. Scalapino, Phys. Rev. B **78**, 020514(R) (2008).

[21] K. Seo, C. Fang, B.A. Bernevig, and J. Hu, Phys. Rev. B **79**, 235207 (2009).

[22] A.D. Christianson, E.A. Goremychkin, R. Osborn, S. Rosenkranz, M.D. Lumsden, C.D. Malliakas, L.S. Todorov, H. Claus, D.Y. Chung, M.G. Kanatzidis, R.I. Bewley, T. Guidi, Nature **456**, 930 (2008); M.D. Lumsden, A.D. Christianson, D. Parshall, M.B. Stone, S.E. Nagler, G.J. MacDougall, H.A. Mook, K. Lokshin, T. Egami, D.L. Abernathy, E.A. Goremychkin, R. Osborn, M.A. McGuire, A.S. Sefat, R. Jin, B.C. Sales, D. Mandrus, Phys. Rev. Lett. **102** 107005 (2009).

[23] S. Chi, A. Schneidewind, J. Zhao, L.W. Harriger, L. Li, Y. Luo, G. Cao, Z. Xu, M. Loewenhaupt, J. Hu, and P. Dai, Phys. Rev. Lett. **102**, 107006 (2009); S. Li, Y. Chen, S. Chang, J.W. Lynn, L. Li, Y. Luo, G. Cao, Z. Xu, and P. Dai, Phys. Rev. B **79**, 174527 (2009).

[24] D.S. Inosov, J.T. Park, P. Bourges, D.L. Sun, Y. Sidis, A. Schneidewind, K. Hradil, D. Haug, C. T. Lin, B. Keimer, V. Hinkov, Nature Phys. **6**, 178 (2010).

[25] T. Hanaguri, S. Niitaka, K. Kuroki, and H. Takagi, Science **328** 474 (2010).

[26] R.M. Fernandes, and J. Schmalian, Phys. Rev. B **82**, 014521 (2010); A.B. Vorontsov, M.G. Vavilov, and A.V. Chubukov, Phys. Rev. B **81**, 174538 (2010).

[27] S. Onari, H. Kontani, and M. Sato, Phys. Rev. B **81**, 060504(R) (2010); S. Onari and H. Kontani, arXiv:1105.6233 (unpublished); arXiv:1107.0748 (unpublished).

[28] Y. Nagai, and K. Kuroki, Phys. Rev. B **83**, 220516(R) (2011); arXiv:1106.2376 (unpublished).

[29] I. Eremin, D.K. Morr, A.V. Chubukov, K.H. Bennemann, and M.R. Norman, Phys. Rev. Lett. **94**, 147001 (2005).

[30] J.-P. Castellan, S. Rosenkranz, E. A. Goremychkin, D. Y. Chung, I. S. Todorov, M. G. Kanatzidis, I. Eremin, J. Knolle, A. V. Chubukov, S. Maiti, M. R. Norman, F. Weber, H. Claus, T. Guidi, R. I. Bewley, and R. Osborn, arXiv:1106.0771 (unpublished)

[31] Y. Qiu, W. Bao, Y. Zhao, C. Broholm, V. Stanev, Z. Tesanovic, Y. C. Gasparovic, S. Chang, J. Hu, B. Qian, M. Fang, and Z. Mao, Phys. Rev. Lett. **103**, 067008 (2009); D.N. Argyriou, A. Hiess, A. Akbari, I. Eremin, M.M. Korshunov, J. Hu, B. Qian, Z. Mao, Y. Qiu, C. Broholm, and W. Bao, Phys. Rev. B **81**, 220503(R) (2010).

[32] We remind that $FeTe_{0.6}Se_{0.4}$ is very different from a parent compound FeTe and shows a metallic behavior in the normal state and a spin response similar to that in Fe-pnictides.

[33] D.J. Singh and M.-H. Du, Phys. Rev. Lett. **100**, 237003 (2008); L. Boeri, O.V. Dolgov, and A.A. Golubov, Phys. Rev. Lett. **101**, 026403 (2008); I.I. Mazin, D.J. Singh, M.D. Johannes, and M.H. Du, Phys. Rev. Lett. **101**, 057003 (2008).

[34] H. Ding, K. Nakayama, P. Richard, S. Souma, T. Sato, T. Takahashi, M. Neupane, Y.-M. Xu, S.-H. Pan, A. V. Fedorov, Z. Wang, X. Dai, Z. Fang, G. F. Chen, J. L. Luo and N. L. Wang, J. Phys.: Condens. Matter **23**, 135701 (2011).

[35] J. Knolle, I. Eremin, A.V. Chubukov, and R. Moessner, Phys. Rev. B **81**, 140506(R) (2010).

[36] see e.g., S.Maiti, M.M. Korshunov, T.A. Maier, P.J. Hirschfeld, and A.V. Chubukov, arXiv:1104.2923(unpublished) and references therein.

[37] L.P. Gor'kov and A.I. Rusinov, Zh. Eksp. Teor. Fiz. **46**, 1363 (1964) [JETP **19**, 922 (1964)].

[38] A.B. Vorontsov, M.G. Vavilov and A.V. Chubukov, Phys. Rev. B **79**, 140507(R) (2009).

[39] see e.g., V. Kogan Phys. Rev. B **80**, 214532 (2009).

[40] D.K. Pratt, M.G. Kim, A. Kreyssig, Y.B. Lee, G.S. Tucker, A. Thaler, W. Tian, J.L. Zarestky, S.L. Budko, P.C. Canfield, B.N. Harmon, A.I. Goldman, and R.J. McQueeney, Phys. Rev. Lett. **106**, 257001 (2011).